

# Comparison of Deghosting Algorithms for Multi-exposure High Dynamic Range Imaging

Kanita Hadziabdic\*

International University of Sarajevo, Bosnia and Herzegovina

Jasminka Hasic Telalovic<sup>†</sup>

International University of Sarajevo, Bosnia and Herzegovina

Rafal K. Mantiuk<sup>‡</sup>

Bangor University, United Kingdom

## Abstract

High dynamic range (HDR) images can be generated by capturing a sequence of low dynamic range (LDR) images of the same scene with different exposures and then merging those images to create an HDR image. During capturing of LDR images, any changes in the scene or slightest camera movement results in ghost artifacts in the resultant HDR image. Over the past few years many algorithms have been proposed to produce ghost free HDR images of dynamic scenes. In this study we performed subjective psychophysical experiments to evaluate four algorithms for removing ghost artifacts in the final HDR image. To our best knowledge, no evaluation of deghosting algorithms for HDR imaging has been published. Thus, the aim of this paper is not only to evaluate different ghost removal algorithms but also to introduce a methodology to evaluate such algorithms and to present some of the challenges that exist in evaluating ghost removal algorithms in HDR images. Optical flow algorithms have been shown to produce successful results in aligning input images before merging them into an HDR image. As a result one of the state-of-the-art deghosting algorithm for HDR image alignment is based on optical flow. To test the limits of the evaluated deghosting algorithms the scenes used in our experiments were selected following the criteria proposed by Baker et al. [2011], which is considered as *de facto standard* for evaluating optical flow methodologies. The scenes used in the experiments serve to provide challenges that need to be dealt with by not only algorithms based on optical flow methodologies but also by other ghost removal algorithms for HDR imaging. The results reveal the scenes for which the evaluated algorithms fail and may serve as a guide for future research in this area.

**Keywords:** high dynamic range imaging, deghosting algorithms

## 1 Introduction

Most real world scenes contain large amount of luminance variation. There is a number of methods for capturing high dynamic range illumination that is present in typical real world scenes. Mitsunaga and Nayar [2000] have proposed a means of capturing HDR content by using specialized hardware. Alternatively, CCD sensors [Wen 1989; Street 1998] may be used to capture HDR values. Commercially only a few companies (e.g. SpheronVR GmbH,

Panoscan MK-3) manufacture HDR cameras and these cameras are extremely expensive for average consumers. The most common and more affordable method of producing HDR images can be done by capturing a sequence of low dynamic range images of the same scene with different exposures and combining those images to produce an HDR image [Mann and Picard 1995], [Debevec and Malik 2008], [Mitsunaga and Nayar 1999], [Robertson et al. 1999a]. However, this approach produces high quality HDR images only for static scenes. Any change in the scene in between each capture of LDR images, or any camera motion will result in the ghost artifacts in the resultant HDR image. As a result, over the past decade a number of algorithms have been proposed to deal with ghost removal in HDR images [Jacobs K 2008], [O. et al. 2009], [Heo et al. 2010], [Zimmer et al. 2011], [Sen et al. 2012]. To our best knowledge, there are no reported psychophysical experiments that compare ghost removal algorithms in HDR images. In this study we perform psychophysical experiments to evaluate the performance of four algorithms in removing ghost artifacts in the final HDR image.

## 2 Related Work

### 2.1 Deghosting algorithms

Over a past decade, several methods that remove ghost artifacts, which may appear as a result of multiple exposure technique of a dynamic scene, have been reported in literature. The simplest approach is to use only one exposure for pixels that contain motion and use all available exposures for pixels that do not contain any motion. This may result in a poor quality HDR image if the scene has large number of pixels that contain both motion and HDR content. Jacobs et al. [2008] used such a technique for ghost removal in HDR images. They first detect pixels that contain motion using entropy and variance. Then, during fusion of LDR images only the pixels from the least saturated LDR image in the detected ghost areas are used by the algorithm. Another method is to align the LDR images to a reference image before combining them to an HDR image. Tomaszewska and Mantiuk [2007] used the homography based approach for image alignment. Assuming only translational misalignment, Akyuz [Akyüz 2011] aligns differently exposed images by using a correlation kernel. Optical flow algorithms are recognized as one of the most successful algorithms in aligning differently exposed LDR images before combining them into an HDR image [Sen et al. 2012]. Zimmer et al. [2011] use state-of-the-art optical flow approach to register LDR exposures before the merging process. They perform image alignment by applying energy-based optical flow approach. They minimize their proposed energy function that uses a data term and a smoothness term to reconstruct saturated and occluded areas. After the alignment, the displacement fields obtained with subpixel precision are used to produce a super resolved HDR image. Their work showed that optic flow approach can successfully be used in HDR reconstruction. Heo et al. [2010] used joint probability density functions between expo-

\*e-mail: kanita@ius.edu.ba

<sup>†</sup>e-mail: jhasic@ius.edu.ba

<sup>‡</sup>e-mail: mantiuk@bangor.ac.uk

sure images to get global intensity transfer functions. Then, during the HDR merging, they applied weighted filtering using the obtained global intensity transfer functions to weigh each exposure. Zhang and Cham [2012] deghosting algorithm is based on gradient directed multi-exposure composition where ghosted areas are detected by examining gradient changes between different exposures. Recently, Sen et al. [2012] proposed state-of-the-art approach in producing ghost free HDR images of dynamic scenes with varying complexity. Their algorithm is based on patch-based energy-minimization formulation. The algorithm iteratively performs joint optimization of image alignment and HDR merge process until all the exposures are correctly aligned to the reference exposure and a good quality HDR result is produced. They achieve this using the HDR image synthesis equation consisting of two terms. The first term of the equation uses information from the reference exposure for pixels that are well-exposed. For poorly exposed areas of the reference image, the second term uses the information from the other exposures through a bidirectional similarity energy term. By this approach, the resultant HDR image uses information from all exposures and is aligned to reference exposure. Detailed review of deghosting algorithms is beyond the scope of this paper. Recent advances in producing ghost free HDR images can be found in [Srikantha and Sidib 2012].

## 2.2 Objective quality metrics

Ideally, we would like to use an objective and computational quality metric to measure how well different deghosting algorithms perform, without the need to run psychometrical experiments. Both simple [?] and complex [?] metrics for HDR images have been proposed, however, none of them is suitable for the evaluation of deghosting algorithms. One of the major reasons is the lack of a well defined reference image for this task. If a series of exposures contain an object in motion, any frame of that motion could be used for the final result. However, a reference image would impose that only one particular pose of the object in motion is a correct solution. Furthermore, deghosting may introduce some geometrical distortions. Objective metrics are very sensitive to small pixel misalignments, while they are often hardly noticeable. Finally, merging JPEG images does not allow to faithfully reconstruct linear scene intensities, even such as those captured in camera's RAW images. This is because of the camera's image processing (tone-mapping), which may vary from one exposure to another. Even small differences in recovery of linear intensity values would result in large errors signalized by most objective quality metrics. For these reasons the results of deghosting algorithms can be evaluated only visually.

## 2.3 Psychophysical experiments

The exploitation of Human Visual System (HVS) knowledge to advance techniques for creation of computer imagery has been heavily explored in computer graphics. A number of papers have used psychophysical experiments to evaluate influence of different features of the graphics imagery.

The influence of senses (such as audio and smell) to the rendering of high-fidelity computer graphics was explored in [?; ?]. The influence of introduction of an additional perception cue (such as sudden movement by an otherwise unsalient object) to the rendering of high-fidelity virtual environments was explored in [?]. In [?] psychophysical experiments have been used to evaluate image retargeting methods used heavily in media. Their results are significant for measures to assess and guide retargeting algorithms.

Psychophysical experiments have also been used for evaluation of HDR imagery techniques. A number of authors have worked on evaluation of tone mapping operators (TMO). These studies have the aim of addressing the problem of displaying the HDR content on LCD monitors. TMOs reduce the dynamic range of the input image to fit the dynamic range of the display. Kuang et al. [2004] carried out psychophysical experiments to test 8 TMOs using 10 HDR images. They tested the overall rendering performance and gray scale tone mapping performance. Ledda et al. [?] performed subjective psychophysical evaluation of 6 tone mapping operators. The experiments involved pairwise comparison of tone mapped images to the reference image displayed on an HDR display. Cadik et al. [2008] evaluated 14 tone mapping methods using basic image attributes. They proposed a measure for the overall image quality based on basic image attributes. They performed subjective psychophysical experiments based on the rating of tone mapped images with reference real world scenes, and ranking of tone mapped images without references to prove the proposed relationship between image attributes. Akyüz et al. [2007] tested whether HDR displays support LDR content. The statistical results of their subjective experiments were surprising. They showed that tone mapped HDR images are no better than the best single LDR exposure. In [?] a psychophysical study of TMOs on small screen devices (SSD) was presented. The obtained results showed that rankings obtained are similar for the LCD and CRT but are significantly different for the SSD.

# 3 Experimental Framework

In our work we performed pairwise comparisons of four deghosting algorithms in HDR imaging. Two of these algorithms are state-of-the-art deghosting algorithms in HDR imaging. The first algorithm is previously mentioned energy-based optic flow approach, proposed by Zimmer et al. [2011]. Zimmer ran his algorithm on our datasets to register the LDR exposures. The second algorithm, also mentioned above is proposed by Sen et al. [2012] and is based on patch-based reconstruction of HDR images. We used publicly available algorithm implementation (in MATLAB code) to run the experiments. Other two algorithms are implemented in the commercially available software packages Photomatix Pro (version 4.2.6) [2012] and Photoshop CS5 Extended (version 12.0).

## 3.1 Experimental scenes

Since algorithm performance may be scene dependent, we took great care to cover a wide range of scenes with varying complexities. In order to test the limits of the evaluated algorithms, the scenes have been selected following the criteria proposed by Baker et al. [2011]. As a result, our dataset consists of complex real-world scenes, with: fast and abrupt motion, high textured motion, independently moving objects, scenes taken with a hand held camera, occlusions, large motion displacement, small motion displacement and stereo sequences of a static scene.

A sequence of three LDR images with different exposures was captured by a digital Canon EOS 1000D camera. All image sizes were reduced (halved) and then cropped to high definition resolution of 1920x1080 for efficient processing by all four evaluated algorithms. Table 1 shows fine-tuning options used to produce HDR (.hdr) images from a sequence of differently exposed LDR images for each of the evaluated algorithms. Whenever possible, we tried to use the options suggested by the authors.

Algorithm name	Options/Fine tuning
Photomatix	Photomatix uses middle exposure as a reference exposure in the HDR merging process. The following pre-processing options were selected as suggested in the Photomatix Manual [?]: <ul style="list-style-type: none"> <li>Align source images check box by matching features with included perspective correction</li> <li>High detection mode for automatically removing ghosts.</li> <li>Reduce noise on all source images</li> <li>Reduce chromatic aberrations</li> </ul>
Photoshop	'Remove ghosts' check box was selected and best reference image was selected manually by the pilot study.
Sen2012	Publicly available MATLAB code was ran with the 'high' quality mode option to produce deghosted HDR image. Middle exposure was used as the reference exposure for all the scenes.
Zimmer2011	Author ran his algorithm on our data sets by selecting middle exposure as reference exposure to register LDR images. We then merged the registered LDR images into HDR image using the Photomatix software.

Table 1: Evaluated deghosting algorithms with the selected fine tuning options.

Since the captured HDR images may contain the dynamic range that is larger than that of a typical display, they need to be tone-mapped. We could use any of the number of proposed tone-mapping algorithms to present the images in the experiment. However, in such a case we run a risk that the tone-mapping may hide the artifacts of the deghosting algorithms. Therefore, instead of more sophisticated tone-mapping operators, we used the "gamma-correction" ( $\gamma = 2.2$ ) contrast compression, which mimics the response of a typical LCD display. Such gamma compression does not distort contrast in any part of the tone-scale, however is prone to clipping the darkest and brightest tones. To minimise clipping in vital image regions, the exposure for each image was selected manually, so that the regions containing artifacts were always visible. In practice, we used *pfsview* HDR image viewer from the *pfstools* package [?] to produce .png images. The resultant image resolution was 1360x758. Figure 5 shows parts of the scenes used in the experiments that may contain ghost artifacts. The scene name shown in the table with bold letters is the name that will be used to refer to the scene throughout the rest of the paper.

### 3.2 Experimental setup

A total of 30 subjects aged between 21 and 47 with computer science background participated in the experiment. All subjects reported normal or corrected to normal vision. We used Psychtoolbox-3 (<http://psychtoolbox.org/>) to design experimental stimuli. All participants were presented with all possible comparison pairs of the same scene processed with a different deghosting algorithm. Let  $n$  be the number of deghosting algorithms used in the experiments, then  $\binom{n}{2} = (n(n-1))/2 = (4 \cdot 3)/2 = 6$  pairs of all possible combinations were presented to a subject for each scene. For a total of eight scenes, each subject was presented with 48 ( $8 \times 6$ )

possible pairs of images. All image pairs were presented randomly for each subject. Also, the screen position of the image within each pair was randomized (i.e. left or right). The experiment setup is shown in Figure 1. Each scene was processed by four algorithms and image pairs were displayed side by side on two 19" Hewlett Packard HP LE1901w LCD monitors. The resolution of each monitor was 1440 x 900 at 60 Hz. Monitors were slightly rotated around the vertical axis (to be perpendicular to the viewing direction) and at an eye level of the subjects, with a viewing distance of 70 cm. All experiments were performed in a darkened room with the same lighting conditions. The only light source was coming from a corridor light. The subjects were asked to choose the preferred image that has the least ghost artifacts for each possible pair. No time limit was imposed in a process of making a choice of the preferred image. One page document with basic concepts on HDR imaging was provided to the subjects before running the experiments. Furthermore, a short lecture on HDR and ghost artifacts was presented. A pilot study was conducted prior to the main study to assess the time needed for each subject to examine and compare the images, to test whether the instructions given to subjects are clear, to determine the viewing distance, etc.

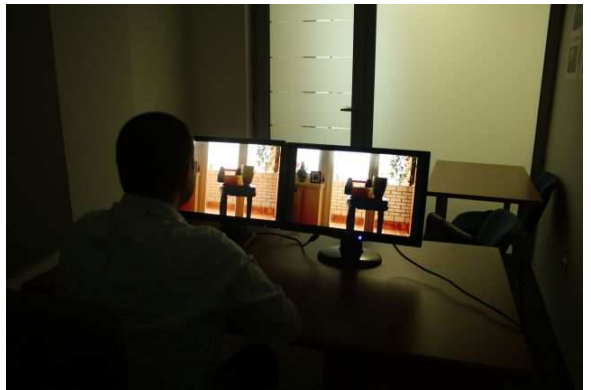


Figure 1: Experimental setup.

## 4 Results and Discussion

The results of the experiment were analysed in two ways: firstly the confidence intervals were established for the number of votes to determine which differences are statistically significant. Secondly, the pairwise comparison data was scaled in Just-Noticeable-Difference (JND) units to stress out the practical significance of these differences.

To determine statistical significance of the differences, we transformed the pair-wise comparison data into the number of votes casted for each deghosting algorithm. The differences in the vote counts between the algorithms were tested for each scene individually using the non-parametric Kruskal-Wallis test. The non-parametric test was used instead of the parametric ANOVA because of the ordinal character of the vote counts. The statistical differences were found for each scene, except **lamplight moving toy**. To test whether the difference between particular algorithms were significant, we performed the multiple comparison test using Tukey's honestly significant difference criterion to adjust for multiple tests. The results of such analysis are shown visually in Figure 3, where the continuous lines denote statistically significant differences and the dashed lines denote the lack of statistical significance at the  $\alpha = 0.05$  level. For the majority of the scenes, we collected sufficient statistical evidence for clear ranking of the algorithms, with

Sen et al. [2012] and Photoshop’s algorithms taking the lead. Note that we do not attempt to average the results over all images because we cannot claim that our set of images is representative for the entire population of possible scenes that can be captured with the multi-exposure method.

The vote counts let us establish statistical significance, however, they hide the practical significance of the quality differences. Given a sufficient number of observers, it is possible to establish statistical significance even when the actual difference between two algorithms is very small. The practical differences are better visualised when the results of the pairwise comparison experiments are transformed into JND units (see Figure 4). The difference of 1 JND unit corresponds to 75% of observers selecting one algorithm over another. The differences below 1 JND can be considered of low practical importance as only few observers will be able to spot the difference.

To scale the pair-wise comparison data in JND units, we used the Bayesian method of Silverstein and Farrell [?]. In brief, the method maximises the probability that the collected data explains the experiment under the Thurston Case V assumptions [?, ch. 8]. The optimisation procedure finds a quality value for each animation that maximises the probability, which is modelled by the binomial distribution. Unlike standard scaling procedures, the Bayesian approach is robust to unanimous answers, which are common when a large number of disparate conditions are compared. The results of such scaling are visualized in Figure 4. In the following paragraphs we analyze the results for each individual scene.

**Abrupt motion** This scene was clearly the most challenging in our experiment, with both Photoshop’s and Zimmer2011 methods producing well visible ghosting artifacts (refer to the top row of Figure 4). We did not find statistically significant difference between Photomatix’s and Sen2012 methods.

**Child in highchair** The differences between the methods are much smaller, mostly within 1 JND. All methods performed well for this scene and the lack of statistical evidence does not allow to make clear distinction between the methods. However, upon closer inspection we could observe some blurring and slight ghosting resulting from Photoshop’s method.

**Complex motion discontinuity** Both Photomatix’s and Zimmer2011 methods produced well visible ghosting for the man moving towards the door. No evidence for a difference between Sen2012 and Photoshop’s methods was found.

**High texture motion** Both Photomatix’s and Sen2012 methods produced images without visible artifacts. Ghosting at the moving leaves of the trees could be observed for Photoshop’s and Zimmer2011 methods. The difference between both groups of method was significant and resulted in at least 1 JND quality difference.

**Independent moving objects** Only Zimmer2012 method resulted in ghosting and significant lower quality ratings. No artifacts could be observed for other methods.

**Lamplight moving toy** All methods produced comparable results without visible artifacts. No statistically significant differences could be observed.

**Plant static camera** This was a relatively easy case for most algorithms, which resulted in statistically indistinguishable quality differences. The only exception was the result of Photomatix, which produced a visibly worse image. The lower quality is most probably due to the artifacts that can be seen as dark splotches on the frame of the window.

**Stereo and occlusion** This is probably the most interesting scene,



Figure 2: Examples of artifacts produced by the deghosting methods for the *Stereo occlusion* scene. The top row shows the shortest exposure, which can be considered a reference. While Photomatix produces gray splotches, the method of Sen et al. generates a texture in the window area.

in which all tested algorithms failed. The algorithm of Zimmer2011 produced very strong ghosting artifacts. Some ghosting, though in lesser amount, could be also found in the result of Photoshop. Photomatix produced ghost-free image, but on closer inspection we found gray splotches in the window area and loss of contrast on the flowers (refer to the middle row in Figure 2). But the most interesting artifact was produced by the algorithm of Sen et al., where in place of the window area a new abstract texture was generated. As shown in the bottom of Figure 2, the texture contained the elements of the scene stitched together, which had little resemblance to the actual view from the windows (top of the figure). This artifact was actually hard to notice without the references as the generated texture looked quite believable.

## 5 Conclusions

In this paper we propose a methodology for evaluating different deghosting HDR algorithms. We used a large variety of scenes and for majority of them we can say, with statistical significance, which algorithms perform better.

The methods that rely on the dense optical flow estimation, such as the method of [Zimmer et al. 2011], perform well for sequences with small continuous motion, but are likely to fail when sequence contains abrupt motion with discontinuities. This is reflected in rather low quality scores for this method. It must be noted, however, that this method involved only spatial alignment and did not use selective weighting of exposures, available to other methods. There is little information available about the deghosting algorithm used in Photoshop, but from our observations, the algorithm seems to fully or partially ignore the exposures that are misaligned rela-

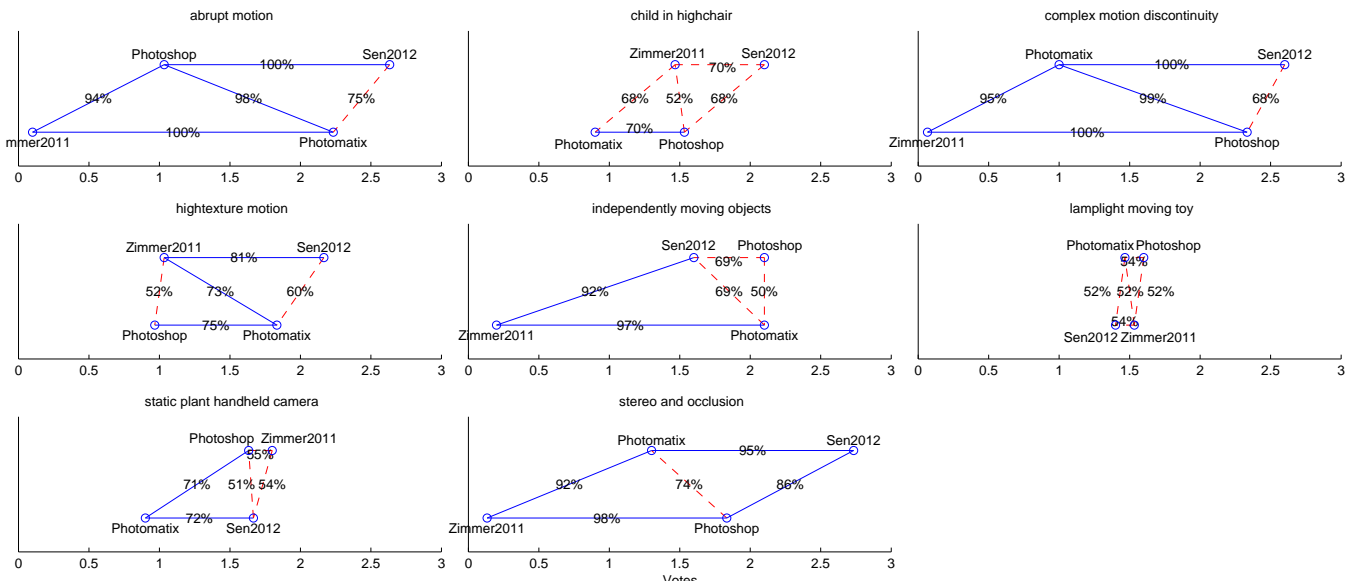


Figure 3: The ranking of the methods and statistical differences. The x-axis represents the average number of votes, where higher number of votes correspond to higher quality. The methods that are connected by the continuous blue lines are statistically significantly different at the significance level  $\alpha = 0.05$ . Such significance cannot be shown for the methods connected by the red dashed lines. The percent numbers on the lines indicate how many observers would judge the method on the right as better than the method on the left.

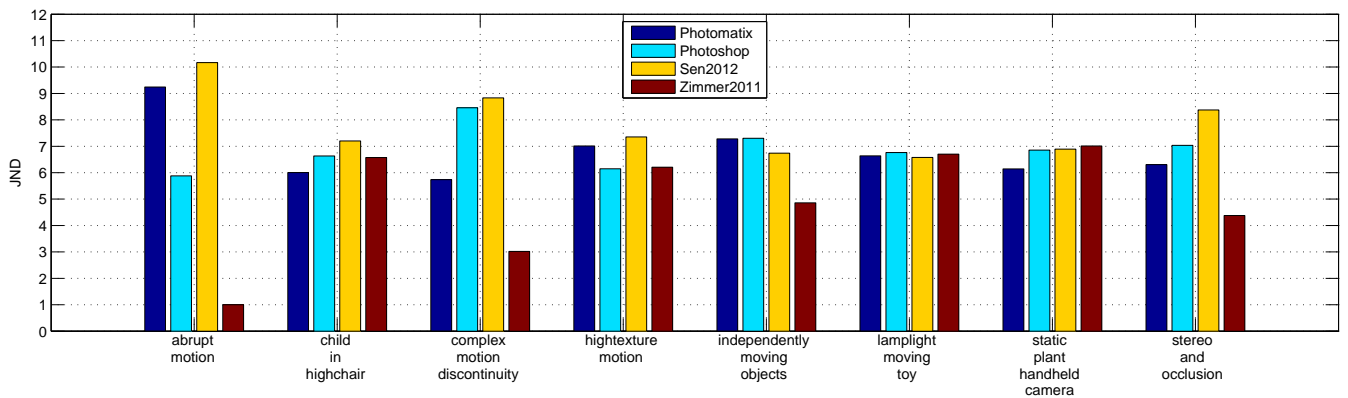


Figure 4: The results of the experiment for each scene scaled in Just-Noticeable-Difference (JND) units. The higher are the values, the higher is the quality. Absolute values are arbitrary and only the relative differences between the methods are relevant.

tive to the reference. The drawback of this approach is the loss of dynamic range in such misaligned regions. The artifacts that could be observed for Photomatrix’s method suggest a spatially adaptive weighting of exposures. These, however, may result in splotchy artifacts. We observed the fewest artifacts in the images produced by the [Sen et al. 2012] method. But even this method struggled in the case of complex motion and low contrast regions (stereo and occlusion scene), which were partially saturated in all exposures.

This study can further be used for improvement of dehazing algorithms specifically focusing on the types of scenes in which current evaluated algorithms did not perform well.

## 6 Acknowledgments

We would like to thank all the participants who participated in our experiments and Henning Zimmer who ran his code on our datasets. This work was partly supported by COST Action IC1005 “HDRi: The digital capture, storage, transmission and display of real-world lighting” and STSM grant COST-STSM-IC1005-10669.

## References

AKYÜZ, A. O., FLEMING, R., RIECKE, B. E., REINHARD, E., AND BÜLTHOFF, H. H. 2007. Do hdr displays support ldr content?: a psychophysical evaluation. *ACM Trans. Graph.* 26, 3 (July).

- AKYÜZ, A. O. 2011. Photographically guided alignment for hdr images. In *Eurographics-Areas Papers*, 73–74.
- BAKER, S., SCHARSTEIN, D., LEWIS, J., ROTH, S., BLACK, M., AND SZELISKI, R. 2011. A database and evaluation methodology for optical flow. *International Journal of Computer Vision* 92, 1–31.
- BANTERLE, F., DEBATTISTA, K., ARTUSI, A., PATTANAIK, S., MYSZKOWSKI, K., LEDDA, P., AND CHALMERS, A. 2009. High dynamic range imaging and low dynamic range expansion for generating hdr content. *Computer Graphics Forum* 28, 8, 2343–2367.
- DEBEVEC, P. E., AND MALIK, J. 2008. Recovering high dynamic range radiance maps from photographs. In *ACM SIGGRAPH 2008 classes*, ACM, New York, NY, USA, SIGGRAPH '08, 31:1–31:10.
- HEO, Y. S., LEE, K. M., LEE, S. U., MOON, Y., AND CHA, J. 2010. Ghost-free high dynamic range imaging. In *ACCV (4)'10*, 486–500.
- JACOBS K, LOSCOS C, W. G. 2008. Automatic high-dynamic range image generation for dynamic scenes. 84–93.
- KUANG, J., YAMAGUCHI, H., JOHNSON, G. M., AND FAIRCHILD, M. D. 2004. Testing hdr image rendering algorithms. In *In: Twelfth Color imaging conference: Color Science and Engineering Systems, Technologies, and Applications*, 315 – 320.
- MANN, S., AND PICARD, R. 1995. "being undigital" with digital cameras: Extending dynamic range by combining differently exposed pictures. In *Proceedings of IS&T 48th annual conference*, 442–448.
- MITSUNAGA, T., AND NAYAR, S. 1999. Radiometric self calibration. In *Computer Vision and Pattern Recognition, 1999. IEEE Computer Society Conference on.*, vol. 1, 2 vol. (xxiii+637+663).
- NAYAR, S., AND MITSUNAGA, T. 2000. High dynamic range imaging: Spatially varying pixel exposures. In *Computer Vision and Pattern Recognition, 2000. Proceedings. IEEE Conference on*, vol. 1, IEEE, 472–479.
- O., G., N., G., W., C., M., T., AND K., P. 2009. Artifact-free high dynamic range imaging. *IEEE International Conference on Computational Photography (ICCP)* (April).
- PHOTOMATIX. 2012. Commercially-available hdr processing software. <http://www.hdrsoft.com>.
- ROBERTSON, M. A., BORMAN, S., AND STEVENSON, R. L. 1999. Dynamic range improvement through multiple exposures. In *In Proc. of the Int. Conf. on Image Processing (ICIP99)*, IEEE, 159–163.
- ROBERTSON, M. A., BORMAN, S., AND STEVENSON, R. L. 1999. Dynamic range improvement through multiple exposures. In *In Proc. of the Int. Conf. on Image Processing (ICIP99)*, IEEE, 159–163.
- SEN, P., KALANTARI, N. K., YAESOUBI, M., DARABI, S., GOLDMAN, D. B., AND SHECHTMAN, E. 2012. Robust patch-based hdr reconstruction of dynamic scenes. *ACM Transactions on Graphics (TOG) (Proceedings of SIGGRAPH Asia 2012)* 31, 6, 203:1–203:11.
- SRIKANTHA, A., AND SIDIB, D. 2012. Ghost detection and removal for high dynamic range images: Recent advances. *Signal Processing: Image Communication* 27, 6, 650 – 662.
- STREET, R. A., 1998. High dynamic range segmented pixel sensor array. US Patent 5789737.
- TOMASZEWSKA, A., AND MANTIUK, R. 2007. Image registration for multi-exposure high dynamic range image acquisition. In *In: Proc. of International Conference in Central Europe on Computer Graphics, Visualization and Computer Vision*.
- WEN, D. D., 1989. High dynamic range charge-coupled device. US Patent 4873561.
- ZHANG, W., AND CHAM, W.-K. 2012. Gradient-directed multi-exposure composition. *Image Processing, IEEE Transactions on* 21, 4 (april), 2318 –2323.
- ZIMMER, H., BRUHN, A., AND WEICKERT, J. 2011. Freehand HDR imaging of moving scenes with simultaneous resolution enhancement. *Computer Graphics Forum (Proceedings of Eurographics)* 30, 2, 405–414.
- ADK, M., WIMMER, M., NEUMANN, L., AND ARTUSI, A. 2008. Evaluation of hdr tone mapping methods using essential perceptual attributes. *Computers and Graphics* 32, 3, 330 – 349.

**Photomatix**



**Photoshop**



**Sen2012**



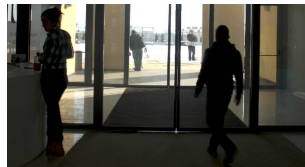
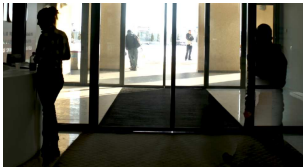
**Zimmer2011**



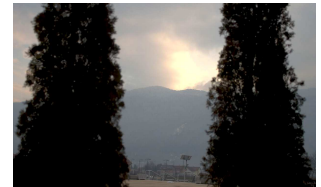
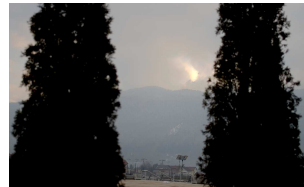
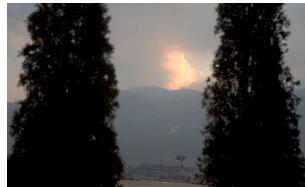
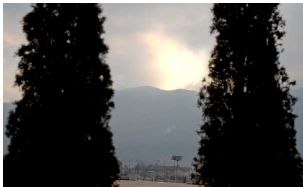
**Abrupt motion:** a complex dynamic scene involving significant and fast abrupt motion, large motion displacement and occlusion. Images were captured with a hand-held camera using automatic exposure bracketing (-2EV, 0EV, 2EV)



**Child in high chair:** a scene with a child in motion captured with a hand-held camera using automatic exposure bracketing (-2EV, 0EV, 2EV)



**Complex motion discontinuity:** a complex dynamic scene containing several independently moving objects, large motion displacement and occlusion. The scene was captured with a hand-held camera using automatic exposure bracketing (-2EV, 0EV, 2EV)



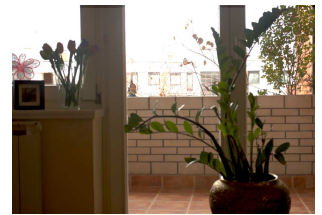
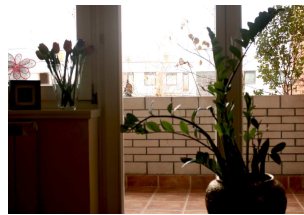
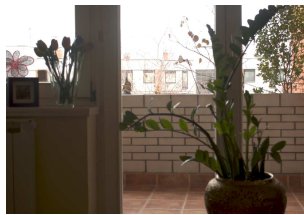
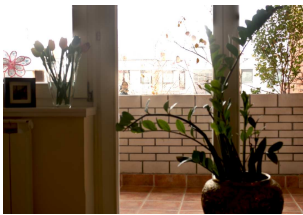
**High texture motion:** a scene that includes high texture motion and small motion displacement. Evergreen trees were moved between LDR capture to simulate motion.



**Independently moving objects:** a scene containing independently moving objects. The objects were moved between LDR capture to simulate motion.



**Lamplight, moving toy:** a scene containing a moving wooden toy with plenty of shadows present in the scene. A wooden toy was moved between LDR capture to simulate motion.



**Static plant:** a static scene captured with a hand-held camera using automatic exposure bracketing (-2EV, 0EV, 2EV)



**Stereo and occlusion:** a stereo sequence of a static scene. Camera was moved between LDR capture.

Figure 5: Images of evaluated algorithm results for all 8 scenes used in the experiments.